Using Abaqus/Explicit to Link the Manufacturing Process to the Final Part Quality for Continuous Fiber-Reinforced Composite Fabrics

Konstantine A. Fetfatsidis, Dimitri Soteropoulos, Alexander Petrov,
Cynthia J. Mitchell, and James A. Sherwood

Department of Mechanical Engineering, University of Massachusetts at Lowell, One University
Ave., Lowell, MA 01854, USA

Abstract: The manufacture of continuous fiber-reinforced composite parts often involves a design-build-test methodology which can be expensive and time-consuming. A predictive design tool, such as the finite element method, is valuable to assist in understanding the relationship between the composite processing conditions and part quality, thus reducing the dependence on the design-build-test methodology. The ability of the design tool to predict part quality based on manufacturing process parameters is dependent upon the mechanical behavior of the fabric reinforcements, which includes the in-plane shearing and tensile behaviors, bending stiffness and friction between contacting surfaces during the manufacturing process. A hybrid finite element discrete mesoscopic approach is proposed to model the forming of continuous fiber-reinforced composite fabrics. The yarns are modeled by 1-D elements, and the shearing behavior of the fabric is incorporated with 2-D elements. Forming simulations are demonstrated using an automotive part and a wind turbine blade, where feedback can be provided to either change processing parameters or part design to optimize part quality.

Keywords: Composites, Design Optimization, Fabrics, Finite Element, Thermostamping.

1.   Introduction

The benefits of continuous fiber-reinforced polymer-matrix composites materials relative to metals are well known, e.g. higher specific strength, higher specific stiffness, corrosion and fire-resistance and tailored energy absorption. Multiple orientations of continuous, aligned fibers are typically woven, knitted, or stitched (often referred to as non-crimp) together in a sheet of fabric. The aerospace, automotive, and wind-energy industries continue to increase their use of these composite materials in an attempt to make lighter, more efficient parts. Processes such as Vacuum Assisted Resin Transfer Molding (VARTM) (Aoki *et al.*, 2010) and thermostamping (Gorczyca *et al.*, 2007)(Wakeman *et al.*, 1998) are capable of producing lightweight quality parts relatively fast with reasonably low processing costs. However, uncertainties in material behavior and in processing conditions result in overdesigned parts that unnecessarily increase weight and costs. Additionally, a time-consuming iterative design-build-test methodology is often used to determine the most efficient design. The cost in time and labor is an obstacle to the widespread use of these aligned-fiber fabric-reinforced composites.

A reliable simulation tool will help to explore the relationship between the processing conditions and the forming of defects such as wrinkles or tearing while maintaining a cycle time that is as

short as possible. In addition, the simulation tool can provide the positions and orientations of the fabric constituents after forming which is of great importance for structural analysis of the formed part. Such structural analyses could include modal analysis, stiffness and damage tolerance.

For a woven fabric and for many non-crimp fabrics, the main mode of deformation at the mesoscopic scale (as opposed to the microscale, i.e. the scale of the fibers) is the in-plane shearing of the fabric, which results in a change of the angle between the initially orthogonal yarns. In a woven fabric, stretching of the fibers as a result of the uncrimping of the yarns is an additional mode of deformation. After the yarns have "stretched" to their limit, then in-plane shearing is the principal mode of deformation during the draping of a three-dimensional (3D) shape. The finite element method is very amenable to the development of a simulation tool for continuous fiber-reinforced fabric composites because it can account for the mechanical behavior of the fabric and the complex boundary conditions (such as the effect of a binder). Geometrical methods such as fishnet draping models do not have this ability and thus are only suitable to simulate handmade draping (Boisse *et al.*, 2008).

In the current work, a discrete approach based on an explicit finite element formulation using a hypoelastic description is demonstrated for simulating the deformation of continuous fiber-reinforced composite fabrics during forming processes. The explicit formulation was chosen because it is the best suited formulation for forming simulations due to its computing time efficiency and relatively robust contact algorithms. In developing this method, the objective was to keep a relatively simple description and to have a scheme that can be implemented within popular commercially available explicit finite element packages that allow for linking of user-defined material subroutines with the explicit solver. To demonstrate this ability, the model was implemented within the commercial explicit code, Abaqus/Explicit.

2.   Model description

A discrete description of the fabric is built using a mesh of 1-D and 2-D elements (Figure 1), where a unit cell represents the yarn interval in the fabric. The 2-D elements account only for the shearing resistance of the fabric and have no tensile or bending stiffness. Appropriate nonlinear constitutive equations deduced from a set of material characterization experiments are associated with the 1-D and 2-D elements via the Abaqus/Explicit user-defined material subroutine, VUMAT, to capture the mechanical behavior of the fabric.
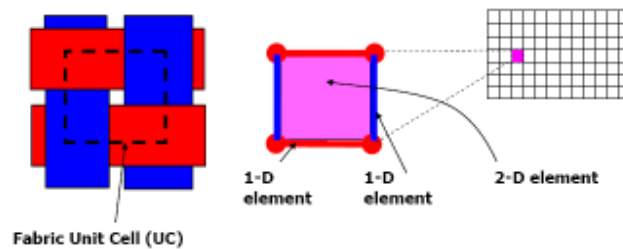

Figure 1. Principle of the discrete mesoscopic modeling using a combination of 1-D and 2-D elements.

Contact between layers of fabric and between the fabric and tooling is defined via the 2-D elements. A constant coefficient of friction is traditionally assumed in forming simulations. However, it has been shown that the polymer matrix in a composite fabric exhibits frictional properties that vary as a function of several process parameters including pressure, velocity, and matrix viscosity (Akkerman *et al.,* 2007) (Chow, 2002) (Fetfatsidis, 2009) (Gamache, 2007) (Gorczyca *et al.*, 2003) (Vanclooster *et al.*, 2008). As a result, it is necessary to use the Abaqus/Explicit user-defined friction subroutine, VFRIC, to implement a variable friction coefficient.

2.1   VUMAT: user-defined material subroutine

To model large deformation and strains, Abaqus/Explicit uses rate-dependent constitutive equations, also called hypoelastic laws. Stresses are updated using the Hughes and Winget formula (Bathe, 1996):

$$\sigma_{ij}^{t+1} = \sigma_{ij}^{t} + \Delta\sigma_{ij}^{t+1} \tag{1}$$

$$\Delta\sigma_{ij}^{t+1} = C_{ijkl}.\Delta\varepsilon_{kl}^{t+\frac{1}{2}} \tag{2}$$

where $\Delta\sigma_{ij}^{t+1}$ is the stress increment at time step *t+1*, C_{ijkl} is the constitutive matrix and $\Delta\varepsilon_{kl}^{t+\frac{1}{2}}$ is the midpoint strain increment obtained from the integration of the strain rate tensor. Abaqus/Explicit allows the user to link custom constitutive models with the overall solver to update the stress (Equation 2) via its user-defined material subroutine, VUMAT. The strain increment, $\Delta\varepsilon_{kl}^{t+\frac{1}{2}}$, is given by the solver to VUMAT that subsequently returns the corresponding stress increment to the solver. The stress update is made in the local reference frame for the element, i.e. a co-rotational frame that rotates with the element (Figure 2). The summation of the strain increments gives a logarithmic (or true) strain in the principal-stretch directions (Abaqus, 2006). Details associated with the constitutive equations as they pertain to the 1-D and 2-D elements are provided in (Jauffres *et al.*, 2009).
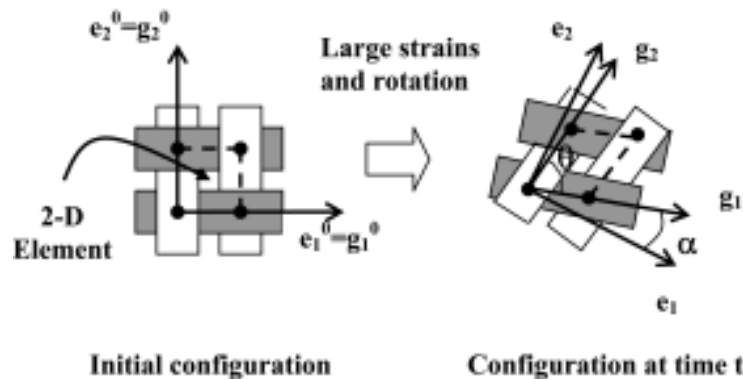
Figure 2. Schematic representation of the different coordinate systems used (Jauffres *et al.*, 2009).

2.2   VFRIC: user-defined friction subroutine

The user-defined friction subroutine, VFRIC, in Abaqus/Explicit allows for the implementation of a variable coefficient of friction between contact pairs. Nodes in contact are referred to as contact points, and a local coordinate system is defined for each contact point to determine the frictional forces and incremental slips (Abaqus, 2006).

During a forming simulation, the incremental frictional slip, or tangential motion during each time increment for each contact point is passed to VFRIC from the Abaqus/Explicit solver. Similarly, the magnitude of the normal force at each contact point is also passed to the subroutine at the end of each time increment. The coefficient of friction is calculated as a function of the tangential motion and the normal force within the subroutine and returned to the solver. The calculation of the friction coefficient depends upon an experimental characterization of the frictional behavior and the development of a phenomenological model that relates the nodal velocities and forces to the coefficient of friction.

3.   Material characterization and model validation

Several experiments must be performed to characterize the mechanical behavior of a continuous fiber-reinforced fabric composite and to capture that behavior in the finite element model. These experiments are outlined in (Sherwood *et al.*, 2012). The basic fabric material characterization, presented here, consists of quantifying the evolution of the shear stiffness as a function of yarn rotation and the yarn tensile behavior. For prepreg fabrics, characterization is done over the range of temperatures that can occur during fabric deformation. For dry fabrics, i.e. no prepreg, the characterization can be done at room temperature.

3.1 Shear frame testing

As previously mentioned, shear is the primary mode of deformation experienced by a fabric when it is formed into a part with multiple curvatures. Thus, accurate material characterization is required for modeling of the shear deformation of continuous fiber-reinforced fabrics to obtain a fundamental understanding of the mechanical behavior of the fabric to predict the fabric response during forming processes.

The standard test for measuring the shear behavior of fabrics is the shear-frame test, also known as trellis-frame test, or the picture frame test, as shown in Figure 3. In this test, a fabric specimen is clamped with the yarns typically directed perpendicular and parallel to the four clamping bars. Shear deformation is developed by fixing one corner and applying a tensile load on the opposing corner via a tensile testing machine. The shear angle and the normalized shear force are determined from the machine crosshead displacement and the total load on the frame. Details are given in (Cao *et al.*, 2008).
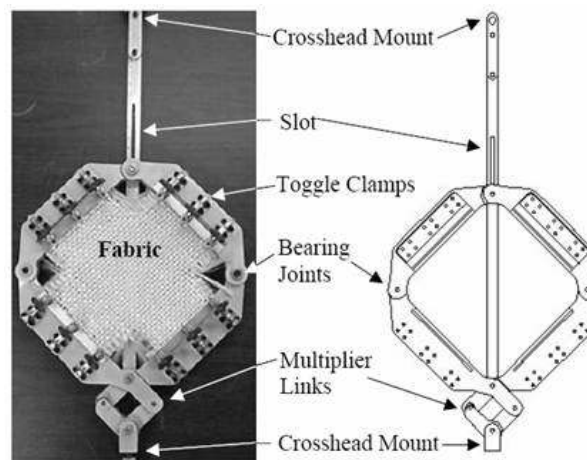

Figure 3. Shear-frame test (Lussier, 2002).

The shear stress as a function of the logarithmic strain is defined within the VUMAT user-defined material subroutine for the 2-D elements in a finite element model of the fabric shear frame test. Figure 4(a) shows good correlation between the normalized shear force versus shear angle curves obtained experimentally and from the Abaqus/Explicit model of the shear frame test. These curves follow the direction of a typical shear deformation curve, as shown in Figure 4(b) with visual depictions of yarn rotation for a woven-fabric composite. The yarns are orthogonal to one another in the initial state. Upon initiation of intraply shear deformation, the yarns begin to rotate and possibly to slip. Yarn slip occurs when two interlaced yarns slide over one another. During yarn rotation, it is assumed that the load is initially due to frictional interaction between adjacent yarns at their crossover points and possibly a viscous contribution if a liquid resin is present. Further deformation continues until an angle is reached where yarn compaction initiates. During

compaction, the adjacent yarns begin to compress each other, increasing the shear stiffness. The locking angle is reached when the yarns are no longer able to compact easily. Deformation beyond the locking angle causes the fabric to buckle out of plane followed by a significant increase in stiffness. At this point, the deformation mode becomes a combination of shear, yarn compaction and tension.
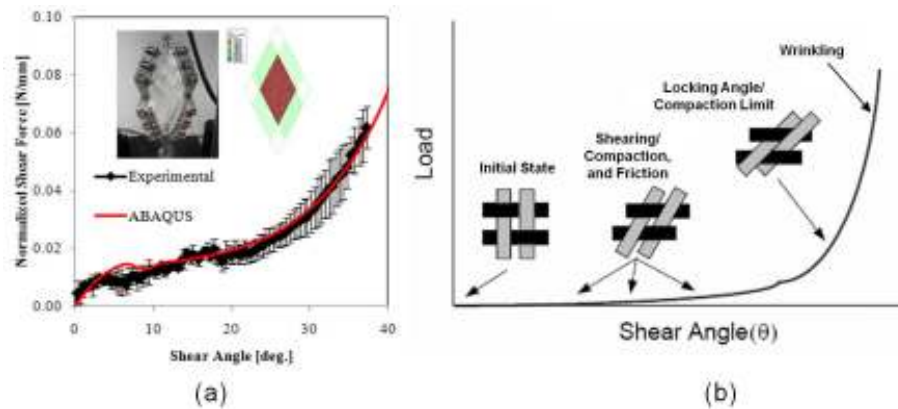

Figure 4. Shear-frame curves showing (a) normalized shear force versus shear angle from experiments and Abaqus/Explicit model and (b) a typical woven-fabric shear behavior curve (Lussier, 2002).

The shear-frame test assumes there is only in-plane pure-shear deformation of the fabric before any out of plane buckling occurs. This assumption has been verified using digital image correlation (DIC). Figure 5 shows a shear-frame test of a plain-weave fabric where DIC has been used to map the state of shear over the surface if the fabric. There is some variation in the shear angle across the surface, but the variation is on the order of ±1°, which can be assumed to be essentially uniform.
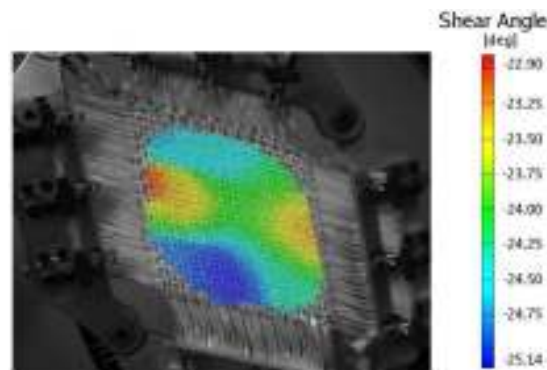

Figure 5. Digital image correlation contours showing pure shear.

3.2 Tensile testing of yarns

As fabric is pressed into a mold, certain yarns may exhibit high tensile stresses as they bridge undulated regions of the geometry, i.e. peaks and valleys. These high tensile stresses can ultimately cause the yarns to break, leading to a poor-quality part. Therefore, to characterize the tensile mechanical behavior of the yarns, uniaxial tensile tests are performed on individual yarns. Pneumatic cord and yarn horn capstan grips are used (Figure 6), and the gage length is set to a relatively high value (~1 m) to minimize the effect of the deformation of the yarn within the grips.

Figure 6. Pneumatic cord and yarn capstan grips. The yarn is wrapped around the horn (1½ turns) and held in place by a pneumatic clamp.

The tensile tests quantify the fracture load and modulus of the yarn (Figure 7(a)). The modulus of the yarn is obtained from the slope of the associated stress/true-strain curve. The effective cross section of the yarn A_{eff} can be determined based on the linear density of the yarn ρ_{linear} and the fiber material density ρ_{mat}:

$$A_{eff} = \frac{\rho_{linear}}{\rho_{mat}} \qquad (8)$$

In addition, the crimp ratio (i.e., the difference between the length of the yarn and the length of the fabric) can be determined for woven fabrics that feature yarn undulations. The combination of the yarn crimp ratio and the yarn modulus is needed to describe the tensile mechanical behavior of a composite fabric (Figure 7(b)).
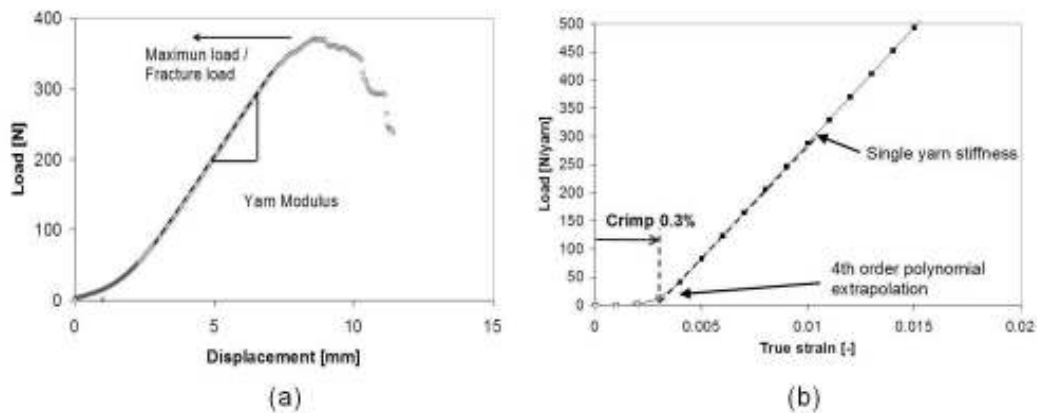
Figure 7. Yarn tensile testing resulting in (a) a typical load-displacement curve and (b) the determination of the fabric tensile behavior from the yarn modulus and the crimp ratio for a typical yarn.

4. Forming simulations

Now that the finite element method has been discussed and its capabilities to capture the complex deformation mechanisms as applied to continuous fiber-reinforced fabrics, simulations of the forming process will be presented. Such simulations can be used to provide feedback regarding the fabric deformation during the forming process and give insight as to if and where defects such as high in-plane shear angles, in-plane and out-of-plane waves and high yarn tensile stresses are developed in the part. With this information, the designer can then reconsider the ply layup so as to achieve the desired structural performance while minimizing the potential for the formation of defects.

In the actual forming process, fabric blanks are initially large enough such that the desired part can be formed. However, after the fabric has been drawn into the mold there will usually be excess fabric around the part that must be removed in an additional step. This excess fabric leads to additional labor, time and waste-material costs. To reduce or eliminate these costs, the simulation can also be used to determine the initial blank shape, or flat pattern, such that little to no excess fabric will remain after being pressed into the mold. A possible approach used to determine the flat pattern consists of first running a simulation with an oversized blank. From the deformed shape of this oversized blank, the "ideal" blank geometry is extracted by deleting the elements associated with the excess material. Then, a second simulation is done to validate the "ideal" blank size. Figures 8 and 9 show the initial and final blank shapes with contours of shear angles (in degrees) for 90/0 and +45/-45 orientations, respectively, using a tooling from an international benchmarking program. This tooling, referred to as the double-dome, was chosen because it includes compound curvatures as depicted by the hemispheres on either end which transition to a trapezoidal trough in the center. The flat sides of the trough allow for the ability to extract test coupons for subsequent material characterization of the cured

composite. Several layers of fabric are initially placed above a stationary cavity and pressed into the mold with a rigid punch.
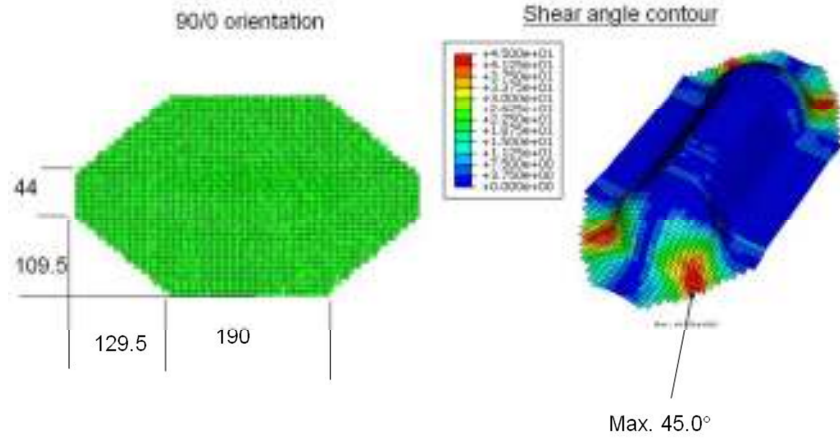

Figure 8. The 90/0 fabric orientation: fabric blank and shear angle contour from the simulation.
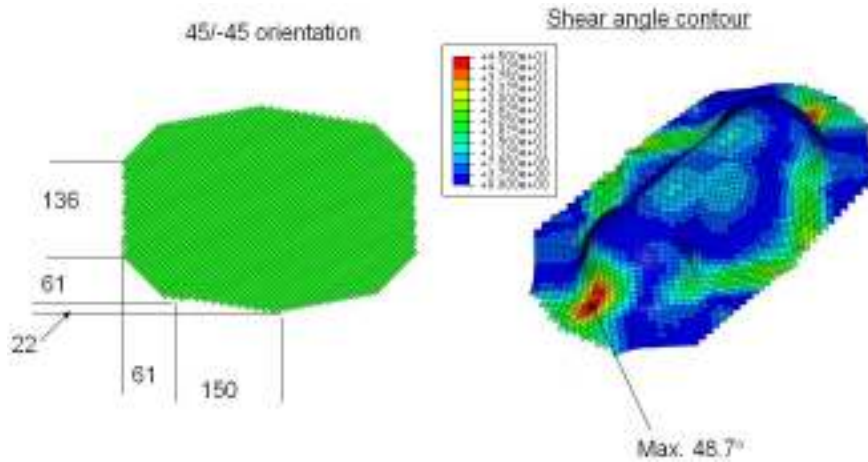

Figure 9. The 45/-45 fabric orientation: fabric blank and shear angle contour from the simulation.

Visual comparisons of yarn orientations can qualitatively evaluate the validity of the modeling. In Figure 10(a), the double-dome stamping of an actual 90/0 sheet (Sherwood *et al.*, 2009) is shown alongside its corresponding finite element model result. The contours shown on the deformed model are the in-plane shear strains in degrees. The overall shapes of the model and the molded part are in good agreement. A zoomed-in view on one quarter

of one hemisphere of the double-dome (Figure 10(b)) confirms the ability of the model to capture the resulting yarn orientation in the molded part. Good agreement is also found between the model and an actual fabric sheet in the -45/45 orientation (Figure 11).
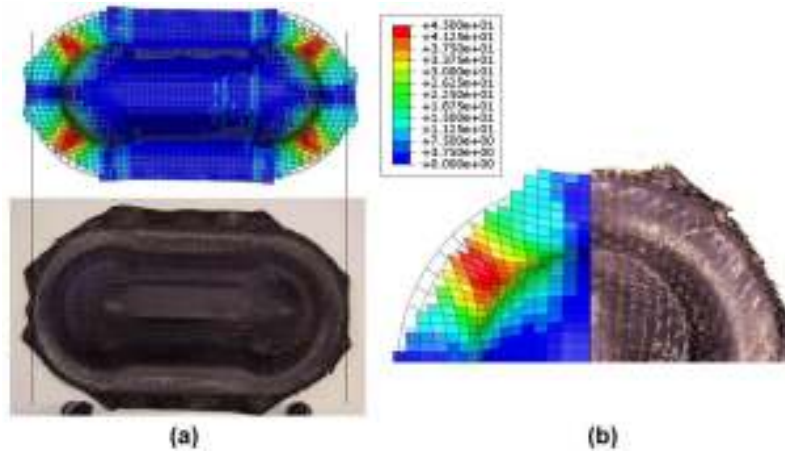

Figure 10. Experimental-simulation comparison of the (a) final shapes for a 90/0 fabric orientation and (b) a quarter of a hemisphere on the double dome
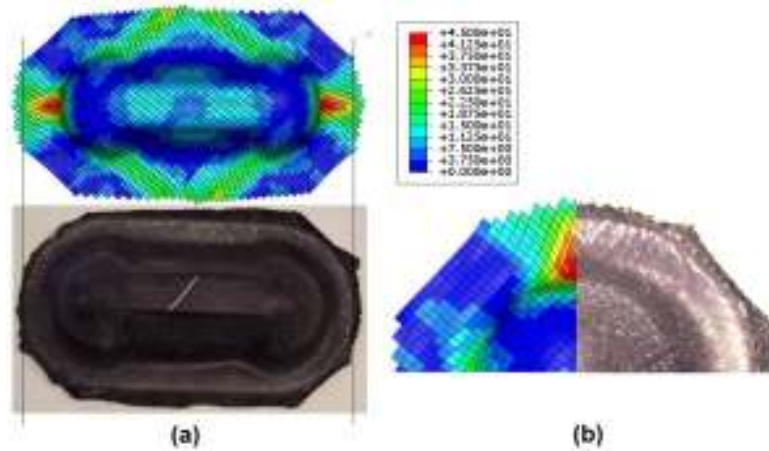

Figure 11. Experimental-simulation comparison of the (a) final shapes for a 45/-45 fabric orientation and (b) a quarter of a hemisphere on the double dome

4.1   Automotive tub

Figure 12 shows the geometry of an automotive rear tub and a floorpan. Forming simulations showed that either the fabric orientations must be changed or the geometry of the tool must be changed to achieve a quality part for these shapes. The ±45° orientation exhibits better drapability to the tub geometry than the 90/0 layout as shown by the lower shear angles in Figure 13(a) (+45/-45) than in Figure 13(b) (90/0). The high shear angles (greater than 60°) in Figure 13(b) suggest the fabric must exceed its "locking angle" to form the shape, at which point the loads may increase beyond the fabric strength, or wrinkling may occur.
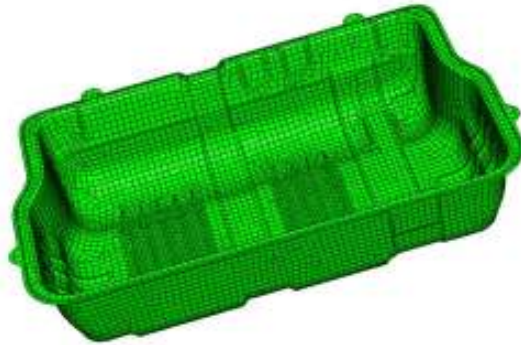

Figure 12. Finite element mesh of the (a) tub punch and the (b) floorpan punch
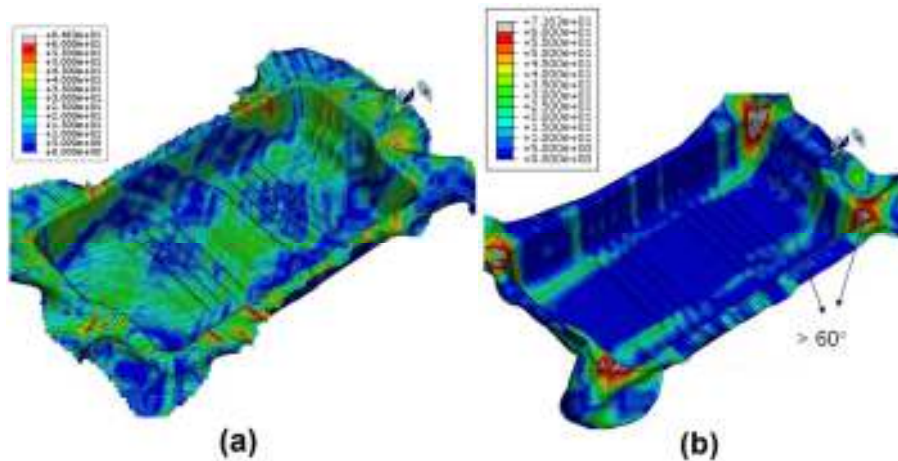

Figure 13. Shear angle contour in degrees (a) for the +45/-45 fabric and (b) for the 90/0 fabric using the tub geometry

As previously mentioned, it is also important for the simulation to be able to predict high tensile stresses in the yarns that may result in yarns breaking and subsequent fabric tearing. The contour of the tension in the yarns is depicted in Figure 14 for the 22.5/112.5 orientation using the tub geometry. High yarn tension at the bottom of the tub can be seen in this figure. The yarn fracture stress could be reached in an actual stamping, leading to fabric tearing in this zone. The high tensile stresses may be a result of the geometry design that features sharp ribs at the bottom. Either the tool design can be changed or smaller patches of fabric can be formed over these areas rather than trying to use one large piece of fabric over the entire part.
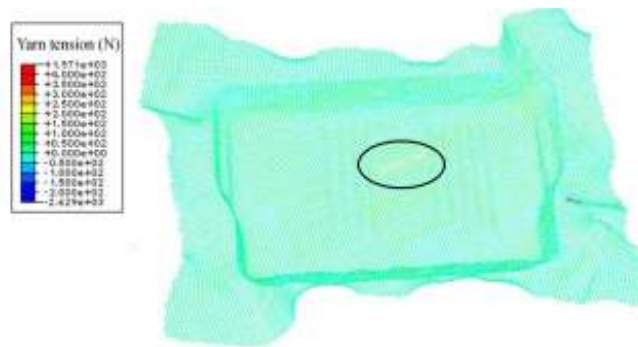

Figure 14. Yarn tension contour for the 22.5/112.5 fabric orientation using the tub geometry. Oval denotes area of high tensile stress in yarns

Molding of the tub confirmed these model predictions, at least qualitatively. The tooling was built before this modeling was done. Molding attempts showed that the 45/-45 plies were able to be formed successfully, but the 0/90 plies were not moldable without significant darting. Note that for structural property reasons, it is not feasible to only mold 45/-45 plies, as part loads will be quasi-isotropic.

4.2   Wind turbine blade

Wind turbine blades are also manufactured using continuous fiber-reinforced fabric composites. It is important that unwanted defects such as in-plane and out-of-plane waviness do not develop during the manufacturing process as these defects may compromise the performance and reliability of the blades. Therefore, this simulation tool is also useful in improving the design and manufacture of composite wind turbine blades.

While the manufacture of wind turbine blades typically involves hand lay-up, the placement of fabric layers can be simulated with the use of a rigid punch, similar to forming processes and these simulations can give guidance in developing automated manufacturing processes. Once the punch has pressed layers of fabric into the mold, an additional pressure can be applied to the surface of the fabric to press each layer tightly into the mold. Figure 15 shows an exploded view of some of the many layers of fabric and core material that constitute a typical composite wind turbine blade.
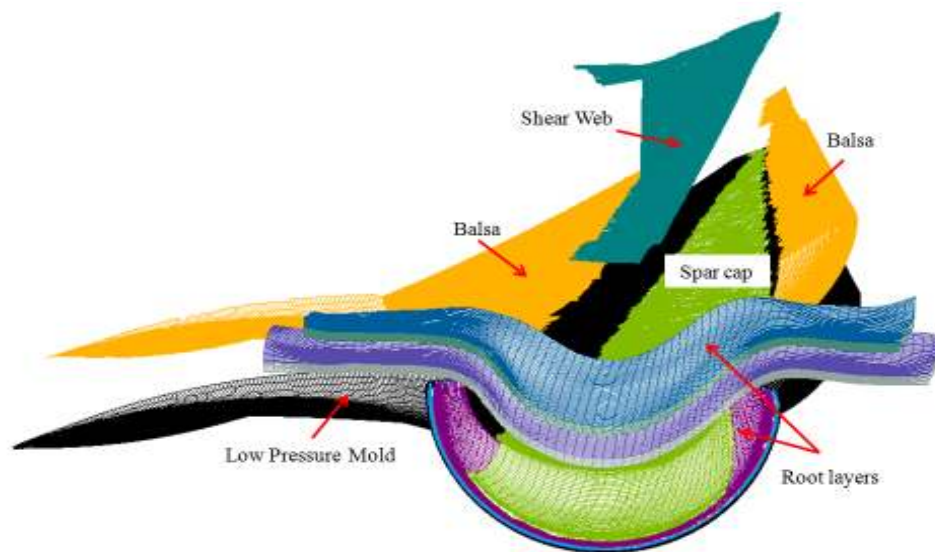
Figure 15. Exploded view of constituents of a 9-meter composite wind turbine blade

Similar to the automotive tub, in-plane shear angles (Figure 16) and yarn tensile stresses (Figure 17) can be observed in sections such as the root of the wind turbine blade to ensure good drapability and that the yarns are not in jeopardy of tearing.
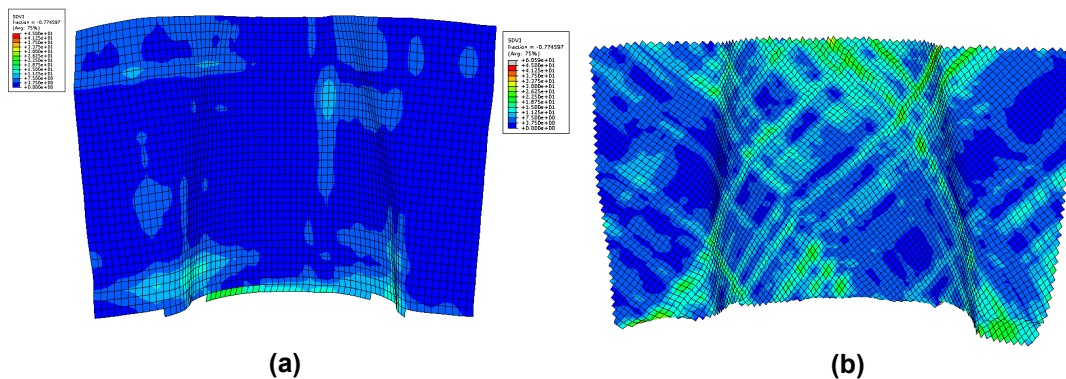

(a)   (b)

Figure 16. In-plane shear angle contours in a (a) 0/90 fabric layer and (b) 45/-45 layer in the root section of a wind turbine blade
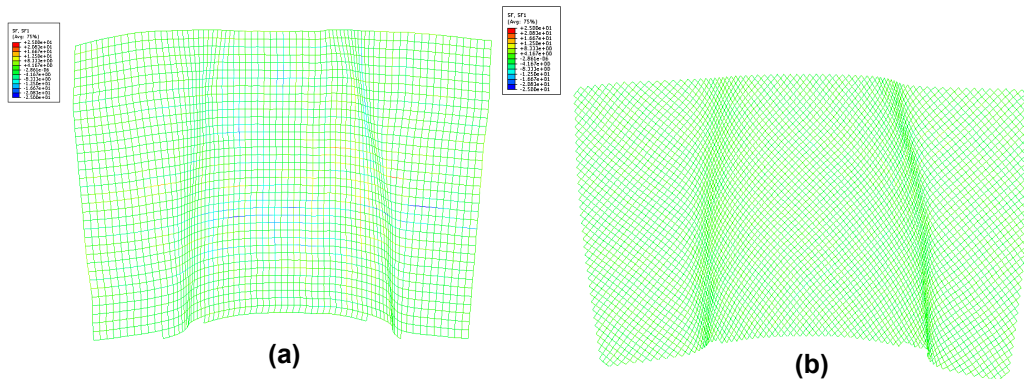
Figure 17. Yarn tensile stresses in a (a) 0/90 fabric layer and (b) 45/-45 layer in the root section of a wind turbine blade

5. Summary

A hybrid finite element discrete mesoscopic approach is used with Abaqus/Explicit to model the forming of continuous fiber-reinforced composite fabrics. The yarns are modeled by 1-D elements, and the shearing behavior of the fabric is incorporated with 2-D elements. Forming simulations are demonstrated using an automotive part and a wind turbine blade, where feedback can be provided to either change processing parameters or part design to optimize part quality.

6. References

1. Abaqus I. Abaqus Theory Manual Version 6.6-1: ABAQUS, Inc., 2006.
2. Akkerman, R., Ubbink, M.P., de Rooij, M.B., and ten Thije, R.H.W.: Tool-Ply Friction in Composite Forming. 10th ESAFORM Conference on Material Forming, 1080-1085, 2007.
3. Aoki Y., Sugimoto S., Hirano, Y., Nagao, Y.: Non-Destructive Inspection Technologies for VARTM Composite Structures. *SAMPE Journal*, 46(1):22-27, 2010.
4. Bathe K. J., Finite Element Procedures. Englewood Cliffs: New Jersey: Prentice Hall, 1996.
5. Boisse P., Hamila N., Helenon F., Hagege B., Cao J.: Different approaches for woven composite reinforcement forming simulation. International Journal of Material Forming, 1:21-29, 2008.
6. Cao, J., Akkerman, R., Boisse, P., Chen, J., Cheng, H.S., DeGraaf, E.F., Gorczyca, J., Harrison, P., Hivet, G., Launay, J., Lee, W., Liu, L., Lomov, S., Long, A., Deluycker, E., Morestin, F., Padvoiskis, J., Peng, X.Q., Sherwood, J., Stoilova, T., Tao, X.M., Verpoest, I., Willems, A., Wiggers, J., Yu, T.X., Zhu.: "Characterization of mechanical behavior of woven fabrics: experimental methods and benchmark results", *Composites: Part A*, **39,** pp. 1037-1053, (2008).
7. Chow S.: Frictional Interaction between Blank Holder and Fabric in Stamping of Woven Thermoplastic Composites. MS Thesis, Department of Mechanical Engineering, University of Massachusetts Lowell, 2002.

8. Fetfatsidis, K.: Characterization of the tool/fabric and fabric/fabric friction for woven fabrics: Static and Dynamic. MS Thesis, Department of Mechanical Engineering, University of Massachusetts Lowell, 2009.

9. Gamache, L.: The Design and Implementation of a Friction Test Apparatus based on the Thermostamping process of woven-fabric composites. MS Thesis, Department of Mechanical Engineering, University of Massachusetts Lowell, 2007.

10. Gorczyca J., Sherwood J., Chen J.: Friction between the Tool and the Fabric during the Thermostamping of Woven Co-Mingled Glass-Polypropylene Composite Fabrics. 18th Annual American Society for Composites Conference, 196-205, 2003.

11. Gorczyca, J., Sherwood, J. and Chen, J.: "Development of a Friction Model for Use in the Thermostamping of Commingled Glass-Polypropylene Woven Fabrics," *Composites Part A*, Vol. 38, p. 393-406, 2007.

12. Jauffres, D., Sherwood, J.A., Morris, C.D., and Chen, J.: "Discrete mesoscopic modeling for the simulation of woven-fabric reinforcement forming" *International Journal of Forming*, Volume 3, Supplement 2, p.1205-1216, 2009.

13. Lussier, D.: Shear characterization of textile composite formability, MS Thesis, Department of Mechanical Engineering, University of Massachusetts Lowell, 2002.

14. Peng, X. Q. and Cao, J.: A continuum mechanics-based non-orthogonal constitutive model for woven composite fabrics. Composites: Part A, 36:859-874, 2005.

15. Sherwood, J.A., D., Jauffres, D., Fetfatsidis, K., and Winchester, D. "Mesoscopic Finite Element Simulation of the Compression Forming of Sheet Molding Compound Woven-Fabric Composites", SPE ACCE Conference, Troy, MI (2009).

16. Sherwood, J.A., Fetfatsidis, K.A., Gorczyca, J.L., Berger, L.: Handbook of Polymer Matrix Composite Manufacturing – Advani & Hsiao, Chapter 19: Fabric thermostamping, Woodhead Publishing, 2012.

17. Vanclooster, K., Lomov, S.V., and Verpoest, I.: Investigation of interply shear in composite forming. Proceedings for the 11th ESAFORM Conference on Material Forming. Lyon, France pp. 957-960. 2008.

18. Wakeman M., Cain T.A., Rudd C.D., Brooks R., Long A.C.: Compression moulding of glass and polypropylene composites for optimised macro and micro-mechanical properties. 1 Commingled glass and polypropylene. *Compos Sci Technol* 58:1879–1898, 1998.

19. Wilks, C.E.: Characterization of the Tool/Ply interface during forming. Ph.D Dissertation, School of Mechanical, Materials, Manufacturing Engineering and Management, University of Nottingham, UK, 1999.

7. Acknowledgements

2012 SIMULIA Community Conference
15